Human Pathology (2019) **91**, 52–60

ELSEVIER

Human PATHOLOGY

www.elsevier.com/locate/humpath

Original contribution

Clear cell papillary renal cell carcinoma: molecular profile and virtual karyotype ☆,☆☆

Diana M. Morlote, MD [a,*,1], Shuko Harada, MD [a,1], Denise Batista, PhD [b], Jennifer Gordetsky, MD [c,1], Soroush Rais-Bahrami, MD [d,e,1]

[a] *Department of Pathology, University of Alabama at Birmingham, Birmingham, AL 35233, USA*
[b] *Johns Hopkins University School of Medicine, Baltimore, MD 21205, USA*
[c] *Department of Pathology, Vanderbilt University Medical Center, Nashville, TN 37232, USA*
[d] *Department of Urology, University of Alabama at Birmingham, Birmingham, AL 35233, USA*
[e] *Department of Radiology, University of Alabama at Birmingham, Birmingham, AL 35233, USA*

Received 15 March 2019; revised 26 May 2019; accepted 31 May 2019

Keywords:
Clear cell papillary renal cell carcinoma;
Genetic profile;
Molecular study;
VHL mutations;
Virtual karyotyping;
Low-grade renal cell carcinoma

Summary Clear cell papillary renal cell carcinoma (CCP-RCC) is a recently recognized tumor that shares morphologic features of both clear cell renal cell carcinoma and papillary renal cell carcinoma but behaves in a more indolent fashion. To date, there is little molecular information available on CCP-RCC. DNA was extracted from formalin-fixed, paraffin-embedded tissue blocks of 22 cases of CCP-RCC at the University of Alabama at Birmingham. Targeted next-generation sequencing and single-nucleotide polymorphism array were performed on all cases. Next-generation sequencing analysis found 30 somatic variants across 63.3% of cases. Seventeen variants (56.7%) were predicted to be deleterious or possibly/probably damaging. Single-nucleotide polymorphism array analysis found copy number abnormalities and/or loss of heterozygosity in 22.7% of cases. We analyzed the genetic characteristics of a group of CCP-RCCs cases and found them to be genetically different from one another. Some cases were genetically similar to clear cell renal cell carcinoma.

1. Introduction

Renal cell carcinomas represent a diverse and ever-expanding group of malignant tumors of the renal cortex with distinct morphologic, genetic, and clinical features. Clear cell papillary renal cell carcinoma (CCP-RCC) is a more recently recognized tumor that, as its name suggests, shares morphologic features of both clear cell renal cell carcinoma (CC-RCC) and papillary renal cell carcinoma (P-RCC). However, despite its morphologic overlap with other entities, this tumor

☆ Competing interests: The authors have no conflicts of interest to declare.

☆☆ Funding/Support: This study was funded in part by the University of Alabama at Birmingham, Department of Urology Junior Faculty Research Award granted to S. R.-B. The rest of the funding was provided by the Adams Grant supported by Robert B. and Jean G. Adams Foundation awarded to D. M. M.

* Corresponding author at: Department of Pathology, University of Alabama at Birmingham, 1802 6th Avenue South, Birmingham, AL 35249.
E-mail address: dmorlote@uabmc.edu (D. M. Morlote).

[1] Authors with equal contribution.

https://doi.org/10.1016/j.humpath.2019.05.011
0046-8177/

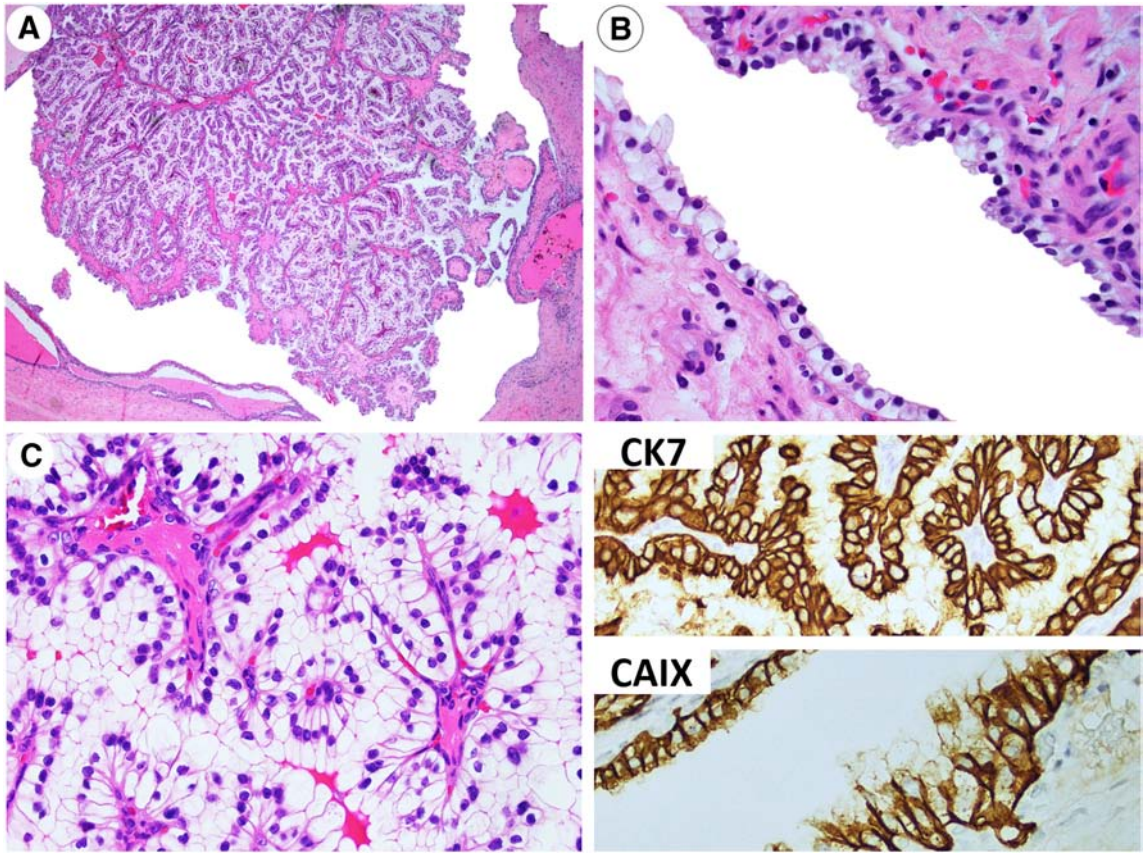

Fig. 1 Case 9: representative case of CCP-RCC. A, Encapsulated neoplasm with delicate papillary projections (original magnification ×40). B and C, Low nuclear grade and nuclei that line up with luminal (reverse) polarity (A-C: hematoxylin and eosin, ×200). IHC stains revealed that CK7 is strong and diffuse. CAIX is strong with fading of the stain on the luminal membrane (both ×200).

has been recognized to have distinct features of its own. CCRCCs are well circumscribed with a well-defined fibrous capsule and are composed of a mixture of cystic and papillary components. The papillae can have densely packed secondary branching, giving the appearance of a solid component. The cells covering the papillae are small to medium sized and cuboidal with small, uniform nuclei that face the luminal surface (reverse polarity) [1]. On immunohistochemistry, tumor cells show strong, diffuse positivity for cytokeratin (CK) 7 and a cup-like staining pattern for carbonic anhydrase (CA) IX, which has been thought to be unique to this entity [2-4]. From a clinical standpoint, CCP-RCC has been seen to arise spontaneously as well as in patients with end-stage renal disease (ESRD) and may favor patients of African descent [5]. In addition, CCP-RCC is thought to behave in an indolent manner.

Currently, the mainstay treatments for renal cell carcinoma include radical nephrectomy or nephron-sparing surgery, such as partial nephrectomy or thermal ablative techniques. However, the last 2 decades has seen an increased aging population in the United States as well as an increase in overall patient co-morbidities. At the same time, there has been an increase in the incidental detection of small renal masses (<4 cm) because of the increased utilization of imaging techniques [6]. As such, the concept of active surveillance, which has been used in other malignancies, is now considered an oncologically safe option in select patients with small renal masses with indolent behavior [7]. Given the different treatment options, being able to classify distinct renal tumors and their associated clinical risk appropriately becomes increasingly important.

The genetics of CCP-RCC have been previously studied in small numbers of cases using conventional karyotype [8], comparative genomic hybridization [9,10], short tandem repeats [11], fluorescence in situ hybridization [12,13], and Sanger sequencing [14]. The presence of *VHL* mutations in sporadic cases of CCP-RCC is a matter of debate. A 2015 study using Sanger sequencing identified *VHL* mutations in 3 of 27 cases of CCP-RCC (11%) [14]. Three unpublished abstracts have also reported *VHL* abnormalities in these tumors [15-17]. Other authors argue that CCP-RCC, when strictly defined, does not harbor abnormalities in the *VHL* gene [3,18,19]. In addition, CCP-RCC–like tumors have been described in the setting of von Hippel–Lindau (VHL) syndrome. The recent description of these tumors along with their relative low prevalence has resulted in lack of a

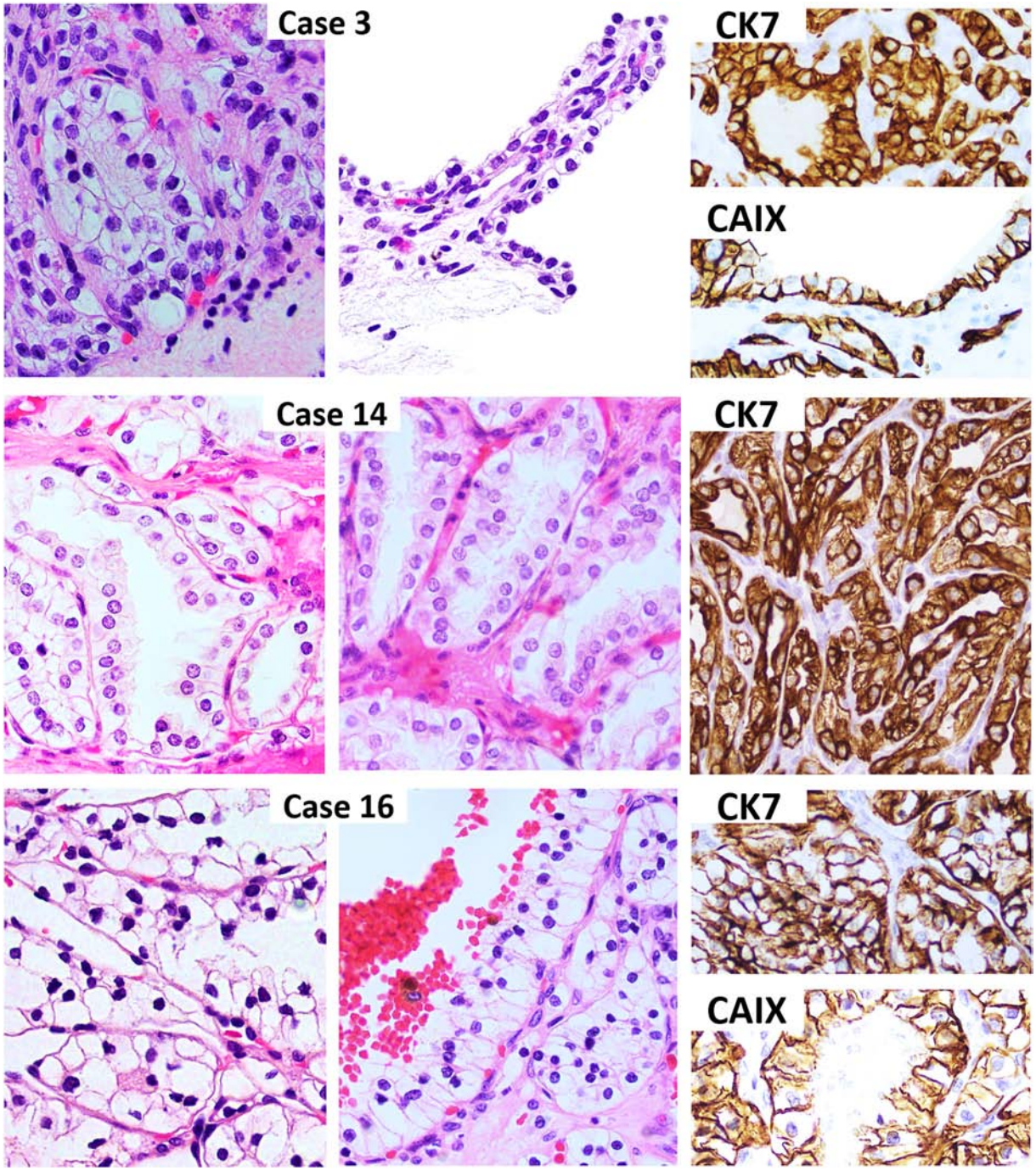

Fig. 2 *VHL* mutation–positive cases. Cases 3, 14, and 16, which harbored *VHL* mutations by NGS, show papillary and microcystic areas with low-grade nuclei that line up with luminal (reverse) polarity, making them morphologically and immunohistochemically indistinguishable from *VHL* mutation–negative cases. CK7 is strong and diffuse. CAIX is strong with fading of the stain on the luminal membrane (all ×400).

comprehensive molecular study of CCP-RCC. We investigated the genetic profile of CCP-RCCs diagnosed and treated at our institution using next-generation sequencing (NGS) and single-nucleotide polymorphism (SNP) array analysis to better understand this newly recognized renal tumor and help distinguish it as a genetically unique entity separate from other renal cell carcinomas.

2. Materials and methods

2.1. Sample cohort

After approval was obtained from the institutional review board at the University of Alabama at Birmingham (UAB), the archive of the Department of Pathology was searched

Table. 1 Clinicopathologic features in 22 cases of CCP-RCC

Case	Sex	Age (y)	Race	Renal comorbidities	Other clinical histories	Tumor side	Tumor size (cm)	ISUP grade	Focality	Tumor stage
1	M	65	AA	ESRD on dialysis	Obesity, HTN, HLD	L	1.3	2	UF	1a
2	M	47	AA	ESRD, APKD, s/p renal transplant	HTN	L	4.5	2	MF	1a
3	M	52	AA	ESRD, s/p renal transplant	HTN	L	0.8	2	UF	1a
4	F	48	AA	ESRD on dialysis	HTN	R	1.2	2	UF	1a
5	F	58	AA	CC-RCC on contralateral kidney	HTN, HLD	L	0.9	2	MF	1a
6	F	71	AA	None	Obesity, HTN	R	2.0	2	UF	1a
7	F	55	AA	None	Obesity, HTN, CAD, stroke, SCD, Hep B	R	3.7	2	UF	1a
8	F	70	AA	None	Obesity, HTN, HLD, DM	R	3.0	2	UF	1a
9	M	67	AA	CC-RCC on contralateral kidney	HTN, CAD s/p MI	R	2.7	2	UF	1a
10	F	50	AA	ESRD, angiomyolipoma	Obesity, HTN, DM	L	1.4	2	UF	1a
11	M	57	AA	None	Obesity, HTN, DM	L	2.5	2	UF	1a
12	F	70	W	CKD	Obesity, HTN, Alpha-1 antitrypsin deficiency	L	0.6	2	UF	1a
13	F	71	AA	CKD, B/L CC-RCC	Obesity, HTN, HLD, DM, breast Ca	L	1.4	2	UF	1a
14	M	79	AA	Bilateral renal cystic lesions	HTN, daughter with RCC	L	UK	2	MF	UK
15	M	57	AA	ESRD, ACKD s/p renal transplant	Obesity, HTN, HLD	R	3.6	2	UF	1a
16	F	50	W	None	Obesity, DM, carcinoid	L	3.5	2	UF	1a
17	M	68	W	Renal calculi on right kidney	Obesity, HTN, DM	R	2.0	2	UF	1a
18	M	25	W	Calculus on left kidney	Obesity	L	5.5	1	UF	1b
19	F	54	AA	B/L CCP-RCC + CC-RCC on the right	Obesity, HTN, HLD.	B/L	5.4 (largest)	2	MF	1b
20	F	75	AA	CKD, h/o B/L CC-RCC	HTN, HLP, DM	L	0.4	1	UF	1a
21	F	59	AA	ESRD	Obesity, HTN, Urothelial CA	L	2.3	3	UF	1a
22	M	66	AA	ESRD on dialysis	Obesity, HTN, HLD	R	2.0	2	MF	1a

Abbreviations: AA, African American; ACKD, acute on CKD; B/L, bilateral; CA, carcinoma; CAD: coronary artery disease; DM, diabetes mellitus; F, female; HLD, hyperlipidemia; HTN, hypertension; L, left; M, male; MI, myocardial infarction; MF, multifocal; R, right; RCC, renal cell carcinoma; SCD, sickle cell disease; UF, unifocal; W, white.

for cases with a diagnosis of CCP-RCC. This yielded a total of 22 cases that were reviewed and confirmed to be morphologically and immunohistochemically typical of CCP-RCC as per the World Health Organization (WHO) 2016 classification of tumors of the urinary system and male genital organs [19] (Fig. 1). After review of all hematoxylin and eosin slides and Immunohistochemical (IHC) stains, a formalin-fixed, paraffin-embedded (FFPE) tissue block was selected from each case for molecular analysis.

2.2. NGS analysis and screening of somatic variants

NGS analysis was performed at a Clinical Laboratory Improvements and Amendments–certified Molecular Diagnostic Laboratory at UAB Hospital. Areas in the FFPE blocks with at least 50% tumor purity were selected, and three 1-mm diameter punches were obtained per case. The tissue cores were deparaffinized before DNA extraction by using Deparaffinization Solution (Qiagen, Valencia, CA). Genomic DNA was isolated by incubating in lysis buffer containing proteinase K digestion at 56°C overnight, followed by a 90°C incubation in an optimized buffer (Qiagen), treatment with RNAse A, and automated purification with the QIAamp extraction column in the QIAcube as per manufacturer's instructions. The concentration of extracted DNA was measured using the Qubit 3.0 Fluorometer (ThermoFisher Scientific, Waltham, MA). The 260:280 ratio was measured by the NanoDrop 2000 Spectrophotometer (ThermoFisher Scientific) to determine purity. The quality of the genomic DNA was assessed by calculating the DNA integrity number using the Genomic DNA ScreenTape (Agilent Technologies, Santa Clara, CA). All samples were found to be of adequate quality for sequencing (DNA integrity number $\geq$4/10). Samples were capture enriched for a comprehensive custom

Table 2 NGS and SNP array variants

NGS variants		Case no. (C), tumor purity (T%), and corresponding VAF (%)																					
Gene and variant	(SIFT/ Polyphen 2Hvar)	C	1	2	3	4	5	6	7	8	9	10	11	12	13	14	15	16	17	18	19	20	21	22
		T%	85	80	85	60	60	70	75	70	65	70	85	80	80	70	60	80	75	80	75	85	80	85
AKT2 p.D457G	T/B								45															
APC p.L2039F	D/PD																	51						
ASXL1 p.H633R	T/B			43																				
ASXL1 p.P805T	T/B															39								
ASXL1 p.D905V	NP/B														36							33		
ATM p.E641G	T/B																		50					
ATM p.T2035I	D/PD								3															
ATM p.C2464R	T/PD																	54						
ATM p.V2915M	D/PD														14									
BCOR1 p.S56C	D/PD														31									
BRCA2 p.S976I	NP/NP						31																	
BRCA2 p.E3053G	D/PD																	8						
CALR p.V349I	T/B								39															
CDH1 p.R545L	D/PD												45											
CDKN2A p.A108S	NP/B				6																			
CDKN2A p.R165S	D/NP																						42	
EGFR p.V765M	T/PD				33																			
ERBB2 p.S442L	NP/PD														31									
JAK1 p.Q565*	NP/NP						26																	
KMT2A p.V1234M	D/B																				52			
NF1 p.S1262Y	T/PD																							5
PHF6 p.I33M	T/B																	21						
PIK3R2 p.V54M	D/B																			55				
SETBP1 p.A246T	T/B								48															
SMC1A p.A73D	D/PD												48											
VHL p.V74G	NP/B																	26						
VHL p.N78S	NP/PD				6																			
VHL p.S80N	D/PD															24								
ZRSR2 p.R448_ R449insSR	NP/NP								10															

NOTE. SNP array data: case 13: +18; case 16: 3p, 3q, 6q, 14q, Xq LOH; case 17: CNC or CN-LOH for chromosomes 1, 2, 3, 4, 6, 7, 8, 9, 10, 11, 13, 14, 15, 22; case 20: CNC or CN-LOH for chromosomes 2, 3, 4, 5, 8, 10, 11, 12, 16, 18, 19; case 22: +3, +12; case 10: many regions with LOH indicating consanguinity. No copy number changes detected in cases 1-12, 14, 15, 18, 19, and 21.
Abbreviations: B, benign; D, deleterious; NP, not provided; PD, possibly damaging; T, tolerated; T%, tumor purity.

cancer panel of 90 genes commonly mutated in cancer (Supplementary Table 1) using the Agilent HaloPlex HS (Agilent Technologies) targeted sequencing method. The HaloPlex HS PCR technology incorporates greater than 10^6 unique molecular barcodes in the DNA library allowing for identification of duplicate reads, significantly improving base calling accuracy even at low allelic fractions. Probes for all regions of interest were designed by the HaloPlex SureDesign on the Agilent website. NGS was performed using the Illumina MiSeq instrument (Illumina, San Diego, CA). FASTQ files were uploaded into the PierianDX (PierianDX, St Louis, MO) pipeline. Before alignment, SureCall (Agilent Technologies) processed the read sequences to trim low-quality bases from the ends, remove adaptor sequences, and mask enzyme footprints. Files were aligned using Novalign (v 3.04.05; Novocraft, Selangor, Malaysia), and various bioinformatics tools, including SAMtools (v 0.1.19; Broad Institute of MIT and Harvard, Cambridge, MA), VarScan (v 2.3.6; The Genome Institute, St Louis, MO), FreeBayes (v 0.9.21-19-gc003c1e; Boston College, Chestnut Hill, MA), and Pindel (v 0.2.4d; Washington University, St Louis, MO) were used to identify variants. Agilent LocatIt (v 3.5.1.46; Agilent Technologies) was used to identify and remove duplicate reads. Quality metrics, including mapping results, and coverage statistics were obtained using BEDTools (v 2.13.3; University of Virginia, Charlottesville, VA) and SAMTools and generated as a PDF file retrievable from the Clinical Geneticists Workspace (PierianDX).

Depth of coverage of at least 50× was required for variant calling. Substitutions with less than 5% variant allelic fraction (VAF) and small insertions and deletions with less than 10% allelic fraction were excluded. Because no sequencing of paired normal tissue was performed, polymorphisms were

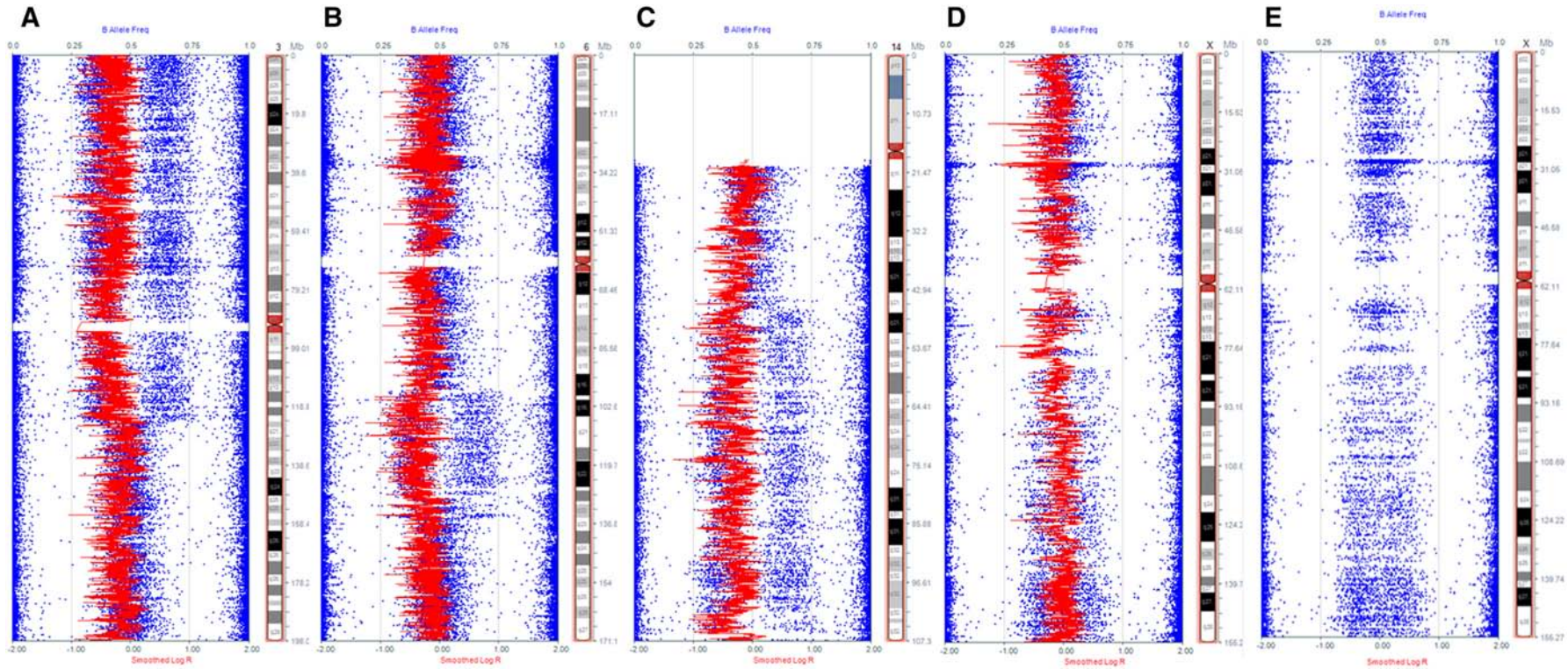

Fig. 3 Case 16: plots showing mosaic loss of the short arm and proximal long arm of chromosome 3 (A), interstitial loss of the long arm of chromosome 6 (B), terminal loss of the long arm of chromosome 14 (C), and terminal loss of the long arm of chromosome X (D). B-alleles plot for chromosome X is also shown separately to better demonstrate the loss, which is present at a lower percentage of cells as compared with the other chromosome losses (E). Red line represents the smoothed Log*R* ratio (LRR) of signal intensity. Blue dots represent allelic composition of B-allele frequency. LRR is the ratio between the observed and the expected probe intensity, thus indicating copy number. B-allele frequency is the frequency of B alleles at a given SNP.

screened by using the Exome Aggregation Consortium database (ExAC; v1.0, http://exac.broadinstitute.org). Variants with frequencies of ≥1% in the population were excluded.

2.3. Immunohistochemistry

Cases were confirmed via appropriate morphologic characteristics and diffuse, positive immunohistochemical staining with CK7 (Ventana, Tucson, AZ) and diffuse, positive cup-like staining for CAIX (Dako, Rocklin, CA; Fig. 1). A CAIX stain was not available on case 14; however, histologic criteria and CK7 staining were typical of CCP-RCC, and an RCC IHC stain was negative (Fig. 2).

2.4. SNP array analysis

SNP array was performed according to manufacturer's protocol on the Human Infinium CytoSNP beadchip with 850K markers (Illumina) after DNA was restored using Infinium HD FFPE DNA Restore Kit. Data were analyzed with copy number variation (CNV) partition 2.4.4.0 using Human Genome build 37/hg19 (National Center for Biotechnology Information, Bethesda, Maryland).

3. Results

3.1. Clinicopathologic findings

The study includes a cohort of 22 cases of CCP-RCC obtained from the archives at the UAB (Table 1). Two cases (cases 1 and 22) occurred in the same patient on contralateral kidneys 1 year apart. The average age of the patients was 59.7 years (range, 25-79 years). Twelve (57.1%) were female, and 9 (47.6%) were male. Seventeen patients (81%) were African American, and 4 (19%) were white. Sixteen patients (76.2%) had renal comorbidities, including 7 (33.3%) with ESRD, 3 (14.3%) with chronic kidney disease (CKD), 2 (9.5%) with nephrolithiasis, and 5 (23.8%) with history of RCC or concurrent RCC. Other comorbidities included hypertension in 19 patients (90.5%), obesity in 14 (66.7%), and type 2 diabetes mellitus in 7 (33.3%). Thirteen cases (59.1%) occurred on the left kidney, 8 (36.4%) occurred on the right kidney, and 1 patient had bilateral tumors. The average size of the tumors was 2.2 cm (range, 0.4-5.5 cm). Classic histologic appearance with low nuclear grade and papillary and tubular/branching architecture was seen in 21 cases (95.4%), 2 of which were International Society of Urological Pathology (ISUP)/WHO grade 1 (9.1%), and 19 were ISUP/WHO grade 2 (86.4%). One case (4.5%) was ISUP/WHO grade 3 (case 21) and was confirmed to be CCP-RCC by strong and diffuse staining with CK7 and positivity for CAIX in a cup-like pattern. Nineteen cases (90.5%) were stage 1a, and 2 cases (9.5%) were stage 1b. The size and stage of case 14 were not able to be determined because of fragmentation of the tumor.

3.2. Genomic alterations detected on NGS

The NGS analysis demonstrated 30 somatic, nonsynonymous variants across 14 of the 22 cases sequenced (63.3%; Table 2). The average number of alterations per case was 1.4 (range, 0-5), and the median was 1. Sixteen (72.7%) of 22 cases had 0 or 1 variant. Only one recurrent variant was detected in the *ASXL1* gene (p.D905V) in cases 13 and 20. Seven variants (56.7%) were previously reported in the COSMIC database [20,21] (*ATM* p.C2464R, *CDKN2A* p.R165S, *EGFR* p.V765M, *VHL* p.V74G, p.N78S, p.S80N, and *ZRSR2* p.R448_R449insSR), but none were previously reported in CCP-RCC. Seventeen variants (56.7%) were predicted to be deleterious or possibly/probably damaging by either the SIFT or Polyphen algorithms, 10 (33.3%) were predicted to be neutral or tolerated, and 3 (10%) did not have a prediction score. *ATM* and *ASXL1*, the genes with the most variants detected, had each 4 variants across 4 cases (18.2% each). Three cases (13.6%) had *VHL* variants. One potentially actionable variant was identified in the *EGFR* gene (p.V765M).

Five of the 14 cases (3, 7, 13, 16, and 22) had variants at allelic fractions below the expected level for the corresponding tumor purity of the sample, which could represent subclones within the tumor.

3.3. *VHL* variants

VHL variants (*VHL* p.V74G, p.N78S, p.S80N) were detected in cases 3, 14, and 16. All 3 variants were documented in the COSMIC database in CC-RCC, and 1 (*VHL* p.N78S) was also documented in hemangioblastoma and serous cystadenoma of the pancreas. Of note, *VHL* p.N78S in case 3 had a low VAF (6%), which could represent a subclone within the tumor. The 3 cases with *VHL* variants were morphologically consistent with CCP-RCC and ISUP/WHO grade 2 (Fig. 2). All 3 cases demonstrated strong and diffuse staining for CK7. Cases 3 and 16 showed positivity in a cup-like pattern for CAIX. A CAIX stain was not available for case 14, but an RCC IHC stain was negative.

3.4. Genomic alterations detected on virtual karyotype

SNP array analysis found copy number abnormalities and/or loss of heterozygosity (LOH) in 5 (22.7%) of the 22 cases (Table 2, also shown in Fig. 3 and Supplementary Figs. 1-4). These included gain of chromosome 18 (case 13), gain of chromosomes 3 and 12 (case 22), and complex abnormalities in 3 other cases (16, 17, and 20) Two of the cases with *VHL* variants had no copy number alterations detected, whereas 1 case (16) showed complex abnormalities (3p, 3q, 6q, 14q, Xq LOH). Interestingly, cases with no variants detected by NGS failed to show copy number variants. All cases with copy number variants had at least 1 variant detected by NGS.

4. Discussion

We detected 30 nonsynonymous somatic variants in hotspots across 90 genes in 63.3% of cases of CCP-RCC. Although 7 of the variants detected have been reported in other tumor types (COSMIC database), none had been previously reported in CCP-RCC. Our study detected 3 cases (13.6%) with somatic mutations in the *VHL* gene, namely, case 3 (*VHL* p.N78S; reported in 5 cases of CC-RCC and 2 cases of hemangioblastoma), case 14 (*VHL* p.S80N; reported in 16 cases of CC-RCC), and case 16 (*VHL* p.V74G; reported in 3 cases of CC-RCC and 1 hemangioblastoma). The histology and immunophenotype of all 3 cases with *VHL* variants were characteristic of CCP-RCC. The classification of these cases as CCP-RCC is controversial. There is no history of VHL syndrome documented in these patients. The available literature argues that *VHL* abnormalities are not found in CCP-RCC and that finding them in sporadic cases precludes a diagnosis of CCP-RCC [1,3,8-10,18,19,22]. However, that begs the question of how to classify tumors with histology and IHC profiles identical to CCP-RCC but *VHL* mutations, given the fact that their features are not characteristic of CC-RCC either.

One of the main IHC stains used to differentiate CCP-RCC from CC-RCC has been CK7, which has been reported as strong and diffuse in CCP-RCC and focal or negative in CC-RCC. However; a 2019 study by Gonzalez et al [23] looked at the reactivity of CK7 in many renal tumors and found a high rate of focal CK7 positivity in 12 of 15 cases of low-grade CC-RCC. Moreover, they examined *VHL* status to identify a subgroup of 15 renal tumors that were morphologically indistinguishable from CCP-RCC but carried *VHL* abnormalities (mutation, methylation, or loss of 3p heterozygosity). They called this group "clear cell papillary-like RCC". Most of these tumors showed strong and diffuse staining for CK7 (11/15). Their staining pattern with CAIX was not described. The behavior of these tumors that are indistinguishable from CCP-RCC and yet harbor *VHL* abnormalities has not been studied. It is unclear whether they behave like *VHL*-negative CCP-RCC or like low-grade CC-RCC. Further complicating the picture is the description of CCP-RCC-like tumors in patients with VHL syndrome. In one study by Williamson et al [24], the authors describe a group of 14 tumors with morphologic overlap with CCP-RCC. All of these tumors with the exception of 2 cases lacked the characteristic IHC profile (CK7 positivity, characteristic CAIX, negativity for α-methylacyl-CoA racemase and CD10); however, a later study by Rao et al [25] looked at 3 patients with VHL syndrome and CCP-RCC-like tumors and found them to show the same IHC profile as sporadic CCP-RCC in terms of CK7 positivity. That these 3 cases were classified as CCP-RCC based on morphology and IHC profile in spite of being driven by *VHL* abnormalities begs the question of why would *VHL* abnormalities exclude a diagnosis of CCP-RCC in sporadic tumors that are otherwise indistinguishable from *VHL* mutation-negative CCP-RCC cases such as the 3 identified by our study or those described by Gonzalez et al [23].

The genes with the most variants identified were *ASXL1*, a chromatin-remodeling gene [26], and *ATM*, a gene involved in the DNA damage response [27]. *ASXL1* variants were identified in 4 cases (4/22; 18%), including 2 cases that shared the same *ASXL1* p.D905V variant. Interestingly, *ASXL1* mutations were recently reported in P-RCC associated with ESRD [26], and the recently published Cancer Genome Atlas Comprehensive Molecular Characterization of Renal Cell Carcinoma [28], which included data on 843 renal cell carcinomas of the 3 major histologic types, documented variants in the polycomb repressive deubiquitinase complex (*BAP1, ASXL1*) in 12.1% of CC-RCC, 6.8% of P-RCC, and 1.4% of C-RCC. Because there is a known association between CCP-RCC and ESRD, it is interesting that *ASXL1* mutations were also identified in our cohort.

One case (case 3) had one possible actionable mutation in the *EGFR* gene (p.V765M), which has been reported in cases of lung adenocarcinoma and hematopoietic malignancies (COSMIC reference: COSM28603).

Of note, 5 of the 14 cases had variants at allelic fractions below the expected level for the corresponding tumor purity of the sample (Table 2). This may represent either tumor heterogeneity in the form of subclones or tumor progression. For example, case 3, which had a tumor purity of approximately 85%, had a *VHL* p.N78S variant with a VAF of 6%. Another variant in the same case, *CDKN2A* p.A108S was also detected at a VAF of 6%, whereas a third variant *EGFR* p.V765M was detected at 33% VAF. It is possible that the variant in *EGFR* represents the driver mutation, whereas the variants in *CDKN2A* and *VHL* are present in subclones that arose later within the tumor.

SNP array analysis showed copy number abnormalities or LOH in a lower percentage of cases (22.7%). There was no pattern in the types of abnormalities detected. Of the 3 cases with *VHL* variants, 2 showed no copy number abnormalities, whereas 1 (case 16) showed losses of 3p, 3q, 6q, 14q, and LOH of the long arm of the X chromosome.

This analysis reflects the lack of disease-specific variants in CCP-RCC. Most cases showed no copy number variants, and more than half of the cases had at least 1 somatic variant detected by NGS. Interestingly, 2 cases from the same patient (cases 1 and 22) occurring a year apart in different kidneys were genetically different with the first tumor showing no detectable abnormalities, whereas the most recent tumor showed an *NF1* gene variant and gain of chromosomes 3 and 12. Two additional cases (17 and 20) showed possible copy number alterations in chromosome 3, which could not be fully elucidated due to background noise.

5. Conclusions

To date, our cohort represents the largest genetic analysis of CCP-RCC to combine NGS data and virtual karyotyping by SNP array. We have demonstrated variability in the

genomic profile of this entity, bearing the question of whether this tumor, with its unique immunohistochemical, clinical, and morphologic profile, truly represents a single entity or rather a heterogeneous group of tumors sharing common histologic features. A subset of immunohistochemically typical CCP-RCC cases was found to harbor *VHL* abnormalities. Whether this particular subset of CCP-RCC still behaves in a clinically indolent manner or whether they should be relegated to another category (ie, clear cell papillary-like RCC) as described by Gonzalez et al [23] remains to be determined. All cases of CCP-RCC studied proved to be genetically different from P-RCC in that trisomy 7 and 17 are not characteristic features.

Acknowledgments

The authors would like to thank supervisor Gina DeFrank and the rest of the staff at UAB's Molecular Laboratory for their work in sequencing cases for this project.

Supplementary material

Supplementary data to this article can be found online at https://doi.org/10.1016/j.humpath.2019.05.011.

References

[1] Gobbo S, Eble JN, Grignon DJ, et al. Clear cell papillary renal cell carcinoma: a distinct histopathologic and molecular genetic entity. Am J Surg Pathol 2008;32(8):1239-45.
[2] Alshenawy HA. Immunohistochemical panel for differentiating renal cell carcinoma with clear and papillary features. Pathol Oncol Res 2015;21(4):893-9.
[3] Rohan SM, Xiao Y, Liang Y, et al. Clear-cell papillary renal cell carcinoma: molecular and immunohistochemical analysis with emphasis on the von Hippel–Lindau gene and hypoxia-inducible factor pathway-related proteins. Mod Pathol 2011;24(9):1207.
[4] Tickoo SK, Reuter VE. Differential diagnosis of renal tumors with papillary architecture. Adv Anat Pathol 2011;18(2):120-31.
[5] Wang K, Zarzour J, Rais-Bahrami S, Gordetsky J. Clear cell papillary renal cell carcinoma: new clinical and imaging characteristics. Urology 2017;103:136-41.
[6] Rais-Bahrami S, Guzzo TJ, Jarrett TW, Kavoussi LR, Allaf ME. Incidentally discovered renal masses: oncological and perioperative outcomes in patients with delayed surgical intervention. BJU Int 2009;103(10):1355-8.
[7] Gordetsky J, Eich M-L, Garapati M, Pena MdCR, Rais-Bahrami S. Active surveillance of small renal masses. Urology 2018;123:157-66.
[8] Wolfe A, Dobin SM, Grossmann P, Michal M, Donner LR. Clonal trisomies 7, 10 and 12, normal 3p and absence of VHL gene mutation in a clear cell tubulopapillary carcinoma of the kidney. Virchows Archiv 2011;459(4):457.
[9] Adam J, Couturier J, Molinié V, Vieillefond A, Sibony M. Clear-cell papillary renal cell carcinoma: 24 cases of a distinct low-grade renal tumour and a comparative genomic hybridization array study of seven cases. Histopathology 2011;58(7):1064-71.
[10] Inoue T, Matsuura K, Yoshimoto T, et al. Genomic profiling of renal cell carcinoma in patients with end-stage renal disease. Cancer Sci 2012;103(3):569-76.
[11] Aron M, Chang E, Herrera L, et al. Clear cell-papillary renal cell carcinoma of the kidney not associated with end-stage renal disease. Am J Surg Pathol 2015;39(7):873-88.
[12] Kuroda N, Shiotsu T, Kawada C, et al. Clear cell papillary renal cell carcinoma and clear cell renal cell carcinoma arising in acquired cystic disease of the kidney: an immunohistochemical and genetic study. Ann Diagn Pathol 2011;15(4):282-5.
[13] Shi S-S, Shen Q, Xia Q-Y, et al. Clear cell papillary renal cell carcinoma: a clinicopathological study emphasizing ultrastructural features and cytogenetic heterogeneity. Int J Clin Exp Pathol 2013;6(12):2936.
[14] Deml K-F, Schildhaus H-U, Compérat E, et al. Clear cell papillary renal cell carcinoma and renal angiomyoadenomatous tumor—two variants of a morphologic, immunohistochemical and genetic distinct entity of renal cell carcinoma. Am J Surg Pathol 2015;39(7):889.
[15] Xu W, Deng F, Melamed J, Zhou M. Incidence and genetic characteristics of clear cell tububopapillary renal cell carcinoma. Mod Pathol 2014;94(27(Suppl 2)):270A.
[16] Behdad A, Monzon F, Hirsch M, et al. Relationship between sporadic clear cell-papillary renal cell carcinoma (CP-RCC) and renal angiomyoadenomatous tumor (RAT) of the kidney: analysis by virtual-karyotyping, fluorescent in situ analysis and immunohistochemistry (IHC). Mod Pathol 2011;91:179A.
[17] Martignoni G, Brunelli M, Segala D, et al. VHL mutation, VHL methylation, chromosome 3p and whole genomic status in clear cell papillary renal cell carcinoma. Mod Pathol 2013;93:233A.
[18] Hes O, Compérat EM, Rioux-Leclercq N. Clear cell papillary renal cell carcinoma, renal angiomyoadenomatous tumor, and renal cell carcinoma with leiomyomatous stroma relationship of 3 types of renal tumors: a review. Ann Diagn Pathol 2016;21:59-64.
[19] Moch H, Cubilla AL, Humphrey PA, Reuter VE, Ulbright TM. The 2016 WHO classification of tumours of the urinary system and male genital organs—part A: renal, penile, and testicular tumours. Eur Urol 2016;70(1):93-105.
[20] Forbes SA, Beare D, Boutselakis H, et al. COSMIC: somatic cancer genetics at high-resolution. Nucleic Acids Res 2016;45(D1):D777-D83.
[21] COSMIC: Catalogue of Somatic Mutations in Cancer [database on the Internet]. 2019 [cited 2019]. Available from: cancer.sanger.ac.uk.
[22] Favazza L, Chitale DA, Barod R, et al. Renal cell tumors with clear cell histology and intact VHL and chromosome 3p: a histological review of tumors from the Cancer Genome Atlas database. Mod Pathol 2017;30(11):1603.
[23] Gonzalez ML, Alaghehbandan R, Pivovarcikova K, et al. Reactivity of CK 7 across the spectrum of renal cell carcinomas with clear cells. Histopathology 2018;74(4):608-17.
[24] Williamson SR, Zhang S, Eble JN, et al. Clear cell papillary renal cell carcinoma–like tumors in patients with von Hippel–Lindau disease are unrelated to sporadic clear cell papillary renal cell carcinoma. Am J Surg Pathol 2013;37(8):1131-9.
[25] Rao P, Monzon F, Jonasch E, Matin SF, Tamboli P. Clear cell papillary renal cell carcinoma in patients with von Hippel–Lindau syndrome—clinicopathological features and comparative genomic analysis of 3 cases. Hum Pathol 2014;45(9):1966-72.
[26] Farooq T, Saeed F, Zhang D, Huang W, Yin C, Zhong M. Whole exome sequencing of end stage renal disease associated papillary renal cell carcinoma (PRCCs). Am J Clin Pathol 2018;149(suppl_1):S144-S.
[27] Pal SK, Ali SM, Yakirevich E, et al. Characterization of clinical cases of advanced papillary renal cell carcinoma via comprehensive genomic profiling. Eur Urol 2018;73(1):71-8.
[28] Ricketts CJ, De Cubas AA, Fan H, et al. The Cancer Genome Atlas comprehensive molecular characterization of renal cell carcinoma. Cell Rep 2018;23(1):313-26 e5.